Integrated Insights from Simulation, Experiment, and Mutational Analysis Yield New Details of LacI Function†

Liskin Swint-Kruse,‡,§,|| Hongli Zhan,||,⊥ and Kathleen Shive Matthews*,§,⊥

Department of Biochemistry and Molecular Biology, MS 3030, The University of Kansas Medical Center, Kansas City, Kansas 66160, and Department of Biochemistry and Cell Biology and W. M. Keck Center for Computational Biology, Rice University, Houston, Texas 77005

Received March 2, 2005; Revised Manuscript Received May 22, 2005

ABSTRACT: Protein structural change underlies many signal transduction processes. Although end-state structures are known for various allosteric proteins, intermediates are difficult to observe. Recently, targeted molecular dynamics simulation (TMD) was used to examine the conformational transition and predict relevant intermediates for wild-type lactose repressor (LacI). A catalog of involved residues suggests that the transition of this homodimer is asymmetric and that K84 is a prominent participant in the dynamic N-subdomain interface. Previous experiments indicated that hydrophobic substitutions at position 84 engender slowed, biphasic inducer binding kinetics, which might reflect the same phenomena observed in TMD. Here, we report biochemical confirmation that DNA and inducer binding remain allosterically linked in K84A and K84L, albeit with a differential smaller than that found in wild-type LacI. Other features of these mutant proteins are consistent with an allosteric conformational shift that approximates that of the wild type. As a consequence, these repressors can be utilized to explore an unanswered question about LacI function: How many inducers (one or two per dimer) are required to diminish operator affinity? The biphasic natures of the K84L and K84A inducer association rates allow direct correlation between the two distinct inducer binding events and operator release. Indeed, the kinetics of operator release for the K84A and K84L closely parallel those for the second inducer binding event. Together with implications from previous equilibrium results for wild-type and mutant proteins, these kinetic data demonstrate that binding of two inducers per dimeric DNA binding unit is required to release the operator in these variant LacI proteins.

The functions of most proteins are not limited to single processes. For example, regulatory proteins must both receive incoming information (frequently via binding a small signaling molecule) and translate this message into an appropriate action (such as altered catalytic rate or binding affinity). Further, the "reception" and "action" sites on a given protein are usually remote in sequence and through space. Thus, the incoming message must travel through a complex network of covalent and noncovalent interactions to reach its target destination. The precise, atom-by-atom mechanism for such allosteric communication remains elusive for even a single protein, and the range of possible mechanisms is as varied as the range of protein folds, perhaps even as large as the number of individual proteins. Our goal is to understand this process in the lactose repressor protein (LacI).[1]

LacI provided one of the earliest examples of a transcriptional regulatory protein (for review, see ref *6*). Each dimer of this tetrameric, bacterial protein binds tightly to a specific sequence of operator DNA to repress transcription of downstream genes. When the nutritional milieu necessitates a change in carbon source to lactose, *Escherichia coli* produces the disaccharide allolactose (*7*). This inducer sugar binds to LacI (two ligands per protein dimer) and elicits a conformational change that is transmitted ∼45 Å through the protein to the DNA binding site, abolishing high-affinity binding and thereby allowing transcription to occur (*6*). Throughout several decades of study, the functional features of this repressor have been described, and quantitative assays have been developed to assess operator and inducer binding, allosteric communication between the two sites, and protein stability (*8*−*13*). Although the structure of LacI proved to be elusive, this impediment was removed by the solution of multiple states of the protein beginning in the 1990s (*2*−*4*, *14*−*18*). Structure availability, advances in molecular dynamics simulations and their application to LacI (*1*, *5*), and detailed biochemical studies of repressor function (*8*−*13*) provide opportunity for more comprehensive study of the allosteric nature of this protein.

One of the residues targeted in all three types of inquiry is lysine 84. This charged side chain is buried in the core N-subdomain interface of the DNA-bound repressor, which

† This work was supported by NIH Grant GM22441 and Robert A. Welch Grant C-576 to K.S.M. L.S.-K. was supported in part by a fellowship from the W. M. Keck Center for Computational Biology (National Library of Medicine Grant LM07093).

* To whom correspondence should be addressed. Telephone: (713) 348-4871. Fax: (713) 348-6149. E-mail: ksm@bioc.rice.edu.

‡ The University of Kansas Medical Center.

§ W. M. Keck Center for Computational Biology, Rice University.

|| These authors contributed equally to this work.

⊥ Department of Biochemistry and Cell Biology, Rice University.

[1] Abbreviations: LacI, lactose repressor protein; IPTG, isopropyl β-D-thiogalactoside; ONPF, *o*-nitrophenyl β-D-fucopyranoside; TMD, targeted molecular dynamics.

10.1021/bi050404+ CCC: $30.25
Published on Web 07/27/2005

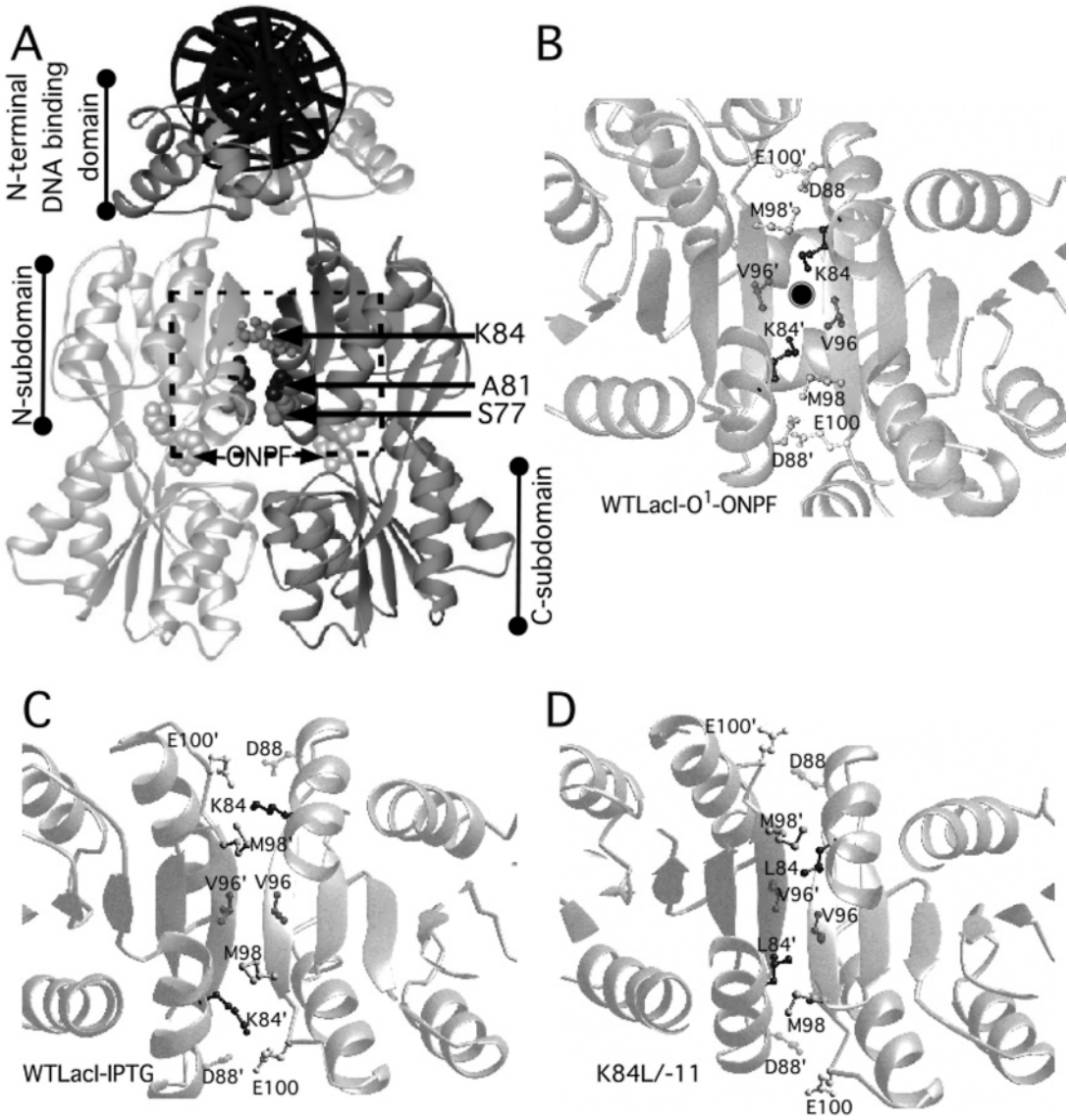

FIGURE 1: (A) Structure of LacI with positions 77, 81, and 84 highlighted. The structure of the dimeric form of LacI bound to DNA (top, black ladder) and anti-inducer, ONPF (gray space-filling representation), is shown. One monomer is colored dark gray and the other monomer light gray. The side chain of A81 is shown as a black space-filling representation, whereas those of K84 and S77 are light gray. The coordinates are from Protein Data Bank entry 1efa (*4*). The protein consists of the N-terminal DNA binding domain, the N- and C-subdomains with the inducer-binding site at their junction, and the C-terminal tetramerization domain (not present in the dimeric structure shown). In the conformational change induced by IPTG, the N-subdomain rotates ~10° and moves along the long axis, propagating conformational change to the N-terminal DNA binding domain and lowering operator affinity (*3*). The protein structure in the dashed box in panel A is enlarged in panels B−D for different LacI structures. (B) Operator/anti-inducer bound (PDB entry 1efa) N-subdomain monomer−monomer interface. The side chain of K84 is inside the hydrophobic environment of the monomer−monomer interface. An adjacent anion (black dot) potentially stabilizes the side chains of K84. (C) Interface of LacI bound to inducer IPTG (PDB entry 1lbh) (*3*). Here, the side chain of K84 is surrounded by hydrophilic side chains of Glu100 and Asp88. New hydrophobic interactions form, such as between V96 and V96′, and further stabilize the interface. The ion in the structure of LacI bound to DNA is removed, and the β-sheets from the two partner monomers move closer together. (D) Interface of K84L/−11 bound to neutral-effector glycerol (PDB entry 1jye) (*22*). Like the interface of LacI bound to DNA (B), the side chain of Leu84 is deeply buried inside the interface, forming extensive hydrophobic interactions. However, the positions of the K84L N-subdomains are more like the wild-type inducer-bound state.

is otherwise a hydrophobic environment (*2*−*4*, *19*) (Figure 1A,B). In the conformation bound to gratuitous inducer IPTG, the K84 side chains move out of the interface and form extensive hydrophilic interactions (*2*, *3*) (Figure 1C). When the LacI conformational change was simulated with targeted molecular dynamics (TMD),[2] movement of the K84 side chain appears to be the juncture between two atomic-level "pathways" that transmit changes through the protein (*5*).

Phenotypic and biochemical properties are well-known for mutations at this position (Table 1): Although charged substitutions have little impact, hydrophobic mutations at position 84 to leucine and alanine drastically slow both association and dissociation for IPTG binding and impart a biphasic nature to the process (Table 1) (*20*). The decrease in both association and dissociation rate constants for these

[2] TMD simulations utilize two different end point conformations of the same protein. Equations of motion are used to drive the structure from one form to the other, thus predicting intermediate dynamics and conformations (*1*). The TMD trajectory of LacI utilized the core domain of the DNA/ONPF-bound dimer and simulated its conversion to the core domain of the IPTG-bound dimer (*2*−*5*).

Table 1: Previously Known Properties of Hydrophobic LacI Interface Variants

	DNA affinity	inducer affinity	inducer binding kinetics	protein stability
K84L	slightly diminished[b]	WT[a,b]	very slow and biphasic[b]	extremely increased[c]
K84A	~WT[b]	WT[b]	slow and biphasic[b]	greatly increased[c]
S77L[d]	very diminished	biphasic	na[f]	na[f]
A81V[e]	very diminished	slightly increased	slow	na[f]

[a] WT = similar to wild-type LacI. [b] From ref *20*. [c] From ref *21*. [d] From ref *46*. [e] From ref *52*. [f] Not available.

Table 2: Previously Known Characteristics of K84L−Glycerol Structure

N-subdomain interface	like wild-type apo-LacI and TMD intermediates (*23*) not like the wild type bound to glycerol or IPTG (*23*)
N-subdomain orientations	like the wild-type complex with DNA and anti-inducer/ONPF (*22*)
K84L side chains	integrated into the hydrophobic interface (*22*)

mutant proteins results in IPTG equilibrium constants similar to that for wild-type LacI (*20*). Although K84L exhibits ~10-fold weakened DNA binding, the affinity of K84A for DNA is similar to that of wild-type LacI. Apolar mutants, K84L and K84A, are significantly stabilized to urea denaturation compared to wild-type protein (*21*) . In fact, tetrameric K84L does not unfold and can even bind IPTG in 6 M urea (*11*). Thus, the side chain at position 84 plays a significant part in the monomer−monomer interface, an observation confirmed upon the solution of the LacI crystal structures (*2*−*4*).

The observed biphasic kinetics for K84 variants may correlate with a major feature found in the TMD simulation of wild-type LacI: asymmetry of intermediate structures in the allosteric conformational change in the LacI homodimer (*5*). Thus, we developed the hypothesis that hydrophobic mutations at position 84 slow the conformational change and allow observation of the proposed biphasic allosteric transition. However, the presence and extent of allostery have never been documented for the K84 hydrophobic variants. In fact, the known structural changes (Table 2) (*22*, *23*) allow the equally viable prediction that allostery is abolished in these variants. We have directly examined communication between the DNA- and inducer-binding sites of K84L and K84A. These data demonstrate that these hydrophobic variants do undergo an allosteric transition, albeit with diminished thermodynamic differences compared to wild-type LacI.

Another long-standing question about LacI is how many inducer molecules (one or two per dimer) are needed to release bound DNA sequences (one DNA/LacI dimer). Taking advantage of the slowed transition in the K84 variants, we designed experiments that yield results supporting the conclusion that two inducer molecules are required to effect the full conformational change to the state with lowered DNA affinity. Finally, results for these and other hydrophobic variants in the N-subdomain interface suggest that a "toggle" between charged and hydrophobic interactions is required to allow wild-type allosteric function in LacI.

MATERIALS AND METHODS

Materials. Unless otherwise specified, all chemicals were purchased from Sigma Chemical Co. (St. Louis, MO). IPTG was from RPI (Troy, NY), urea from Fluka (Milwaukee, WI), and polynucleotide kinase from NEB (Beverly, MA).

Protein Purification. The gene encoding LacI with K84L or K84A and/or −11 (which terminates assembly at dimer) mutations is carried on the pJC1 plasmid (*24*). Protein was expressed in BLIM bacterial cells (*25*) grown in 2× YT media overnight at 37 °C in a shaking incubator. After the cells were harvested by centrifugation, the cell pellet was resuspended with a small amount of lysozyme and frozen at −20 °C, as described previously (*24*, *26*, *27*). The frozen cells were thawed, lysed, treated with DNase, and centrifuged. The crude supernatant was subjected to ammonium sulfate precipitation and the resuspended precipitate applied to a phosphocellulose column following dialysis into 0.05 M potassium phosphate, 5% glucose, and 0.3 mM dithiothreitol (pH 7.5) (0.05 M KP) (for dimer) or 0.09 M potassium phosphate, 5% glucose, and 0.3 mM dithiothreitol (pH 7.5) (0.09 M KP) (for tetramer) (*24*, *26*, *27*). Elution was started at 0.12 M KP (for dimer) or with a gradient from 0.12 to 0.3 M KP (for tetramer). Purified protein was stored in elution buffer (~0.18 M KP for tetramer or 0.12 M KP for dimer). Purity was determined to be >95% by SDS−PAGE. Stoichiometric DNA binding assays (*8*, *26*) were used to determine the fraction of active protein, which was generally ≥85%.

UV Difference Spectroscopy. UV difference spectroscopy was performed as described previously (*26*, *28*−*30*). Experiments utilized the inducers IPTG (0.5 mM, final concentration) and melibiose (5 mM, final concentration), as well as glycerol [25% (w/v)]. The protein concentration was 1.3−2 mg/mL, and the buffer was 0.01 M Tris-HCl (pH 7.4) with 0.15 M KCl. Spectra were measured in triplicate on a Varian Cary 50 spectrophotometer, using a 0.25 nm step size with a 1 s average time. The difference spectra were determined by subtracting the average spectrum of the free protein from the average ligand-bound spectrum.

DNA Binding and Operator Release. DNA binding and operator release experiments were performed using the nitrocellulose filter binding assay (*8*, *31*, *32*). Experiments utilized the natural O^1 operator (5′-TGTTGTGTGGAATTGTGAGCGGATAACAATTTCACACAGG-3′, Biosource International, Camarillo, CA) (*33*). The top and bottom strands of operator sequences were hybridized in 70 mM Tris-HCl, 10 mM $MgCl_2$, and 5 mM DTT (pH 7.6) and then labeled at the 5′-end with [^{32}P]ATP using polynucleotide kinase. Labeled operator was purified from free nucleotide using a Nick column (Amersham Biosciences, Uppsala, Sweden).

In the equilibrium binding assays, the operator concentration was generally $\leq 2 \times 10^{-12}$ M; the protein concentration was varied. If present, inducer and anti-inducer concentrations were fixed at 1 mM. Varied buffer conditions are indicated in tables and figure legends. Radioactively labeled

complex retained on the nitrocellulose filters (Schleicher and Schuell, Keene, NH) was quantitated using a Fuji phosphorimager.

Data from affinity experiments were fit with Igor Pro (Wavemetrics**)** to the equation

$$Y_{obs} = Y_{max}\left(\frac{[\mathrm{LacI}]^n}{K_d{}^n + [\mathrm{LacI}]^n}\right) + c \quad (1)$$

where Y_{obs} is the radioactivity measured at a given protein concentration, Y_{max} is the measured radioactivity when 100% of the DNA was complexed to repressor, K_d is the equilibrium dissociation constant, and c is the background radioactivity in the absence of complex formation. The value of the Hill coefficient, n, was either fixed at 1 or allowed to float, in which case the values cluster around 1.

Operator release experiments were started by incubating labeled operator DNA with repressor and then adding varying concentrations of inducer. Nitrocellulose filter binding was used to monitor decreasing levels of bound DNA as the level of inducer was increased (*26*, *34*−*37*). Resulting data were fit with Igor Pro (Wavemetrics**)** to the equation

$$Y_{corr} = Y_{max} - \left(Y_{max}\frac{[\mathrm{IPTG}]^n}{[\mathrm{IPTG}]_{mid}{}^n + [\mathrm{IPTG}]^n}\right) + c \quad (2)$$

Equation 2 is a variation of eq 1 that accommodates decreasing signal as a function of inducer binding. Y_{max} is the maximum change in radioactivity between conditions of zero and saturating inducer; n is the the Hill coefficient. $[\mathrm{IPTG}]_{mid}$ is the concentration of IPTG where 50% release is observed, and c is a constant background radioactivity.

We have executed two versions of the operator release experiment: In the first manifestation, the operator concentration is set at least 10-fold below K_d for this interaction ($\sim 10^{-12}$ M), the repressor concentration is ~80% of that required for maximal DNA binding of an affinity experiment ($\sim 10^{-9}$ M; note this is below the K_d for DNA binding in the presence of inducer), and the inducer concentration centers around the affinity of inducer binding ($\sim 10^{-7}$ to 10^{-4} M) (*26*, *35*, *36*). In this protocol, both DNA-bound repressor and DNA-free repressor bind IPTG. However, the inducer is in vast molar excess of the protein, and IPTG binding by free LacI does not significantly alter the concentration of free ligand available to the LacI−DNA complex. The second experimental design utilizes a saturating DNA concentration, at least 3-fold above the protein concentration (which may be set at any detectable level) and at least 3-fold below the affinity for binding DNA in the presence of inducer (nonspecific binding). Thus, all protein in the reaction is initially bound to operator, and the complex must always bind added inducer (over the same range described above). In both cases, data are analyzed to determine the inducer concentration where 50% release is observed ($[\mathrm{IPTG}]_{mid}$). These two experimental protocols and different incubation times (from 2 to 24 h) yielded similar data for wild-type and mutant proteins. Since K84 hydrophobic variants have less difference in DNA binding affinity in the absence and presence of inducer, protein concentrations were set so that the maximum difference in intensity between DNA binding curves with and without inducer could be obtained. The individual protein concentrations and DNA concentrations are given in the figure legends.

For kinetic measurements of operator release, Eppendorf tubes were treated with 5% milk to prevent protein adsorption. The concentration of BSA in the binding buffer (FBB) was doubled for the same reason. Protein was incubated with a concentration of O^1 ~3-fold greater than the protein concentration for ~50 min. IPTG was subsequently added at varying times, and a pipet tip was used to gently mix the added inducer for several seconds. After incubation, the solutions were filtered simultaneously using a dot-blot apparatus. Retained radioactivity was quantitated via the usual filter binding assay procedure. The data were fit as a single exponential to determine the release rate:

$$y = y_1 + y_2 e^{-k_{obs}t} \quad (3)$$

where y is the observed retained radioactivity intensity at each time point, y_1 is the background, y_2 is the range of retained radioactivity intensity change induced by IPTG binding, and k_{obs} is the observed release rate with t as the time. Experiments were performed at different IPTG concentrations, and the association rate constant was calculated using a linear model:

$$k_{obs} = k_{on}[\mathrm{I}] + k_{off} \quad (4)$$

where k_{obs} is the observed rate, k_{on} is the association rate constant, k_{off} is the dissociation rate constant, and [I] is the IPTG concentration.

An alternative method for monitoring operator binding utilized gel shift experiments (*38*); these experiments allowed the use of very high glycerol concentrations (up to 60%) in ascertaining the effector status of this sugar. The buffer was that used in the filter binding assay with glycerol added. In this method, protein was incubated with O^1 for 20 min before being loaded onto a 10% native PAGE gel. Using a phosphorimager, the position of radioactively labeled O^1 was visualized, identifying free and bound O^1. The data were analyzed in a manner similar to that for the filter binding assay. Betaine with the same osmolarity as glycerol was used as a control for osmolyte effects, and 1 mM IPTG was used as a positive control for induction and operator release. Multiple protein concentrations were employed to generate varied levels of DNA binding.

Effector Binding. IPTG binding is coincident with a decrease in the fluorescence emission intensity above 340 nm (*9*, *30*). We determined that glycerol binding causes a similar fluorescence shift. To monitor effector binding affinity, the protein concentration was fixed at $1.5-5 \times 10^{-7}$ M monomer, and the effector concentration was varied. If DNA was present, its concentration was $1-2 \times 10^{-6}$ M. Buffer components are indicated in the table and figure legends. Experiments were performed using an SLM-Aminco AB2 spectrofluorometer with an excitation wavelength of 285 nm; emission spectra were recorded between 300 and 380 nm. Data were fit to a variation of eq 2, where $[\mathrm{IPTG}]_{mid}$ was changed to the equilibrium dissociation constant, K_d. The Hill coefficient for wild-type LacI binding to inducer IPTG is 1.0 in the absence of DNA but increases in the presence of operator to a value of ~1.5−1.9 (*12*, *39*). Incubation times are 24 h at 4 °C for K84 variants to

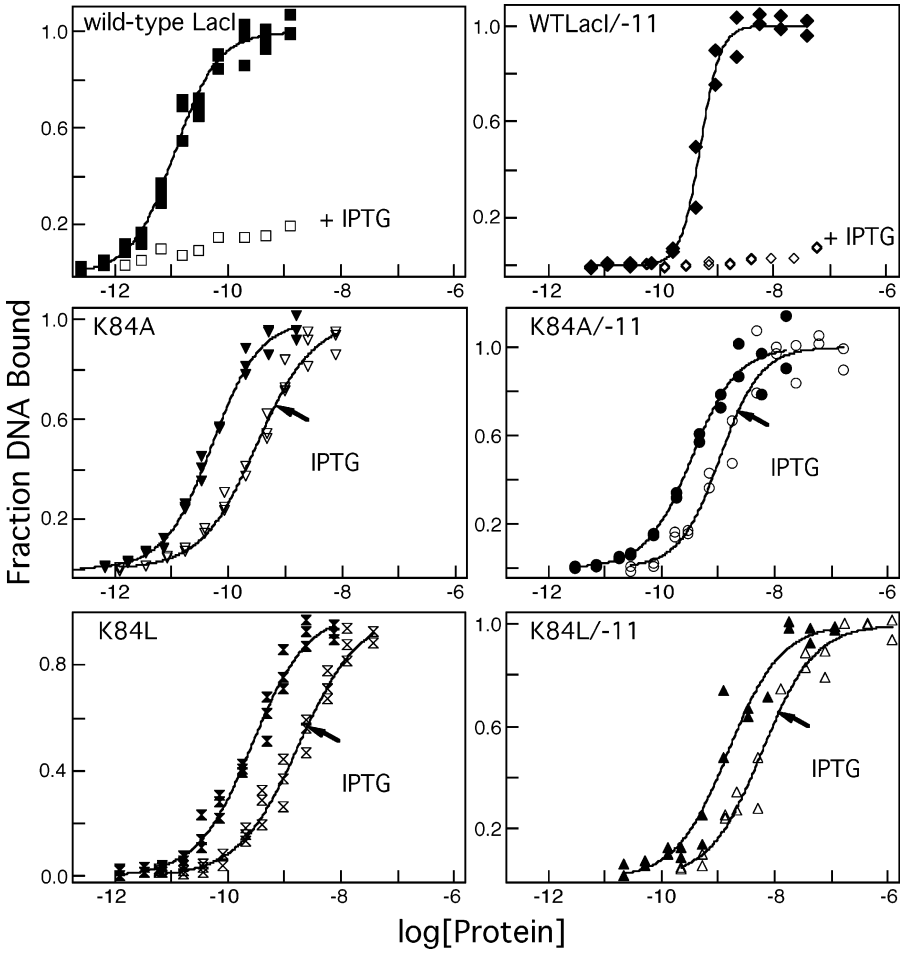

FIGURE 2: Operator binding of wild-type and K84 variants and their dimeric versions in the absence (filled symbols) and presence (empty symbols) of 1 mM IPTG. Experiments were conducted in buffer containing 0.01 M Tris-HCl (pH 7.4), 0.15 M KCl, 0.3 mM DTT, 0.1 mM EDTA, and 5% DMSO. The operator O^1 concentration was 1.5×10^{-12} M. Data shown are for single determinations (triplicate points). Data were analyzed with eq 1, and the results from multiple determinations are summarized in Table 3.

accommodate slowed kinetics in these variants (*20*) and 90 s for wild-type variants.

Kinetic measurements of IPTG binding in the absence of DNA were conducted to ensure repeatability with prior work (*20*). Additional experiments in the presence of DNA measured new parameters for K84A and K84L. The emission spectra in the presence of varying IPTG concentrations were monitored over the time scale shown in the figures. The plot of fluorescence signal intensity versus time was fit using a double-exponential transition to determine two association rates:

$$y = y_1 + y_2 e^{-k_1 t} + y_3 e^{-k_2 t} \quad (5)$$

where y is the fluorescence signal at each time point, y_1 is the background, y_2 and y_3 are the ranges of fluorescence signal change induced by the two binding events, and k_1 and k_2 are the observed association rates for the two binding events with t as the time. Rate constants were obtained from the slope of observed rate versus different IPTG concentration.

Dissociation rate constants were measured by diluting protein·IPTG complexes 20-fold. Protein at 2.5×10^{-6} M (monomer) was incubated with 8×10^{-6} M IPTG for ~30 min to achieve ~80% protein saturation. The dissociation of IPTG from proteins was initiated by diluting the original solution by 20-fold, and the dissociation process was monitored by recording the intrinsic fluorescence change over time on an SLM-Aminco AB2 spectrofluorometer using an excitation wavelength of 285 nm. The emission spectra were recorded between 300 and 380 nm. The plot of fluorescence signal intensity versus time was fit as a double-exponential transition (eq 5) to determine the two dissociation rate constants, where k_1 and k_2 represent the rates for the two dissociation events.

RESULTS

K84 and −11 LacI Variants. Hydrophobic substitutions (leucine and alanine) for K84 have several interesting consequences (Table 1), including diminished, biphasic association rate constants for IPTG binding (*20*). The goal of this work is 2-fold: (1) to determine whether the extent of operator binding is allosterically diminished in response to inducer in a manner similar to that of the wild type and (2) to use the biphasic association kinetics for inducer binding to correlate discrete inducer binding events with operator release.

Most experiments presented in this work make use of the −11 background in directly comparing experiment and structure, which was determined for K84L/−11 (*22*). Wild-type, tetrameric LacI is a "dimer of dimers" (*2*−*4*). A dimeric repressor variant missing the final 11 amino acids ("−11") retains all the functionality of the tetramer except for looping

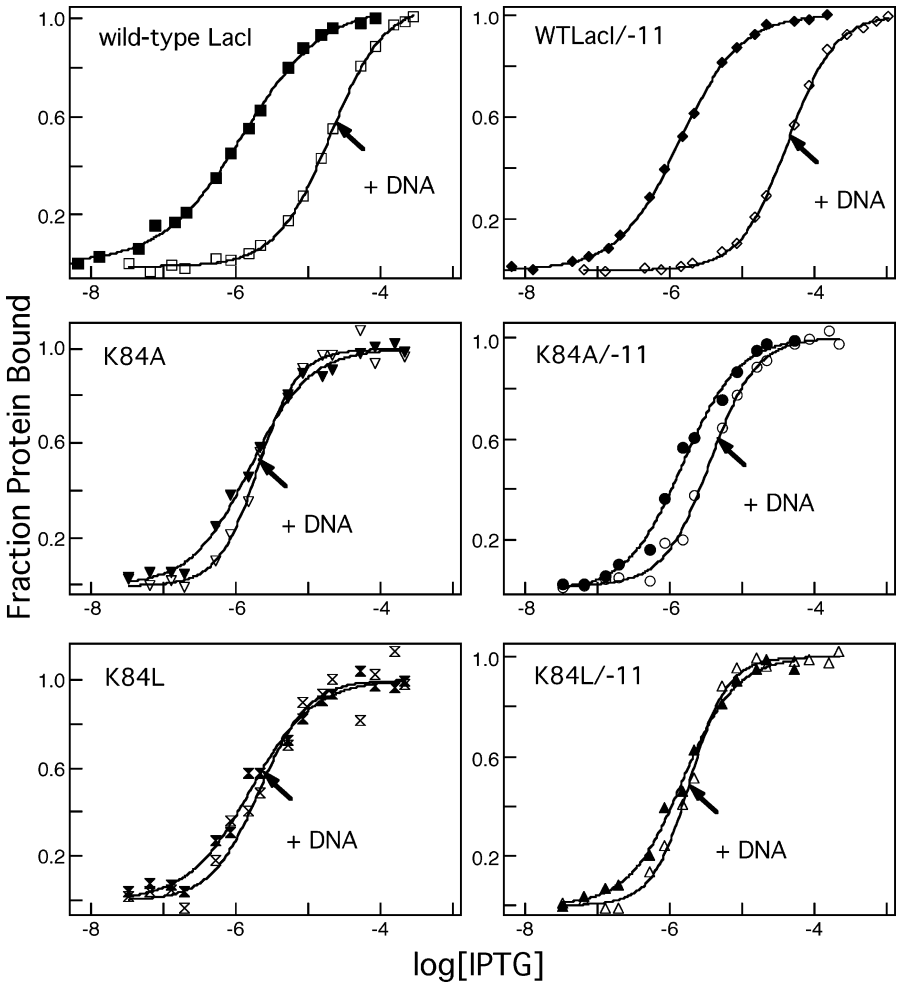

FIGURE 3: IPTG binding of wild-type and K84 variants and their dimeric versions in the absence (filled symbols) and presence (empty symbols) of operator O^1. Experiments were conducted by monitoring fluorescence as described in Materials and Methods in a buffer containing 0.01 M Tris-HCl (pH 7.4) and 0.15 M KCl. The protein concentration was 1.5×10^{-7} M in monomer in the absence of operator and 5×10^{-7} M in the presence of operator. The operator O^1 concentration was 1.5×10^{-6} or 2×10^{-6} M. Data are shown for single determinations. Data were analyzed with eq 2, and the results from multiple determinations are summarized in Table 4.

(simultaneously binding two operator sites on the same strand of DNA) (*6*, *24*, *40*−*42*). Inducer binding for the −11 variant is identical to that for the tetramer (*24*), consistent with the observation that each inducer-binding site is fully contained within the monomer (*43*). Truncated LacI dimers can dissociate to monomers at the low concentrations needed for equilibrium DNA binding measurements, thus increasing the apparent, but not the intrinsic, K_d (*10*). Therefore, some experiments utilize full-length tetramer to eliminate any possible dimer dissociation at low LacI concentration (see below).

Ligand Binding by K84 Variants. Before launching new experiments with the K84 variants, we performed a number of controls under different solution conditions so that our results could be standardized and interpreted in the context of previous work. Binding to O^1 operator DNA was examined for both dimeric and tetrameric LacI and K84 variants (Figure 2 and Table 3). Results are concordant with earlier measurements that indicate a diminished *apparent* affinity of dimeric variants (see above) and ~10-fold lower affinity for K84L than for wild-type LacI (*10*, *20*, *21*, *24*). The difference between tetrameric and dimeric species is diminished for the K84 variants due to the enhanced stability of the monomer−monomer interface conferred by these hydrophobic substitutions (*21*). As previously established, wild-type and variant proteins that were examined exhibit similar affinity for IPTG (Figure 3 and Table 4).

Table 3: DNA Binding by K84 Variants[a]

	K_d ($\times 10^{11}$ M)			
	native	with IPTG	with ONPF	+IPTG/−IPTG ratio
WT	1.5 ± 0.4	>10000	0.9 ± 0.01	>1000
K84A	3.3 ± 0.8	22 ± 2	1.9 ± 0.4	6.7 ± 1.6
K84L	23 ± 3	110 ± 5	15 ± 2	4.8 ± 0.6
−11	63 ± 10	>10000	33 ± 3	>1000
K84A/−11	24 ± 10	120 ± 20	5.8 ± 3	5.0 ± 2.1
K84L/−11	110 ± 30	480 ± 200	48 ± 10	4.4 ± 1.3

[a] Standard deviations shown represent a minimum of three measurements and up to six measurements. Buffer was FBB [0.01 M Tris-HCl (pH 7.4), 0.15 M KCl, 0.3 mM DTT, 0.1 mM EDTA, and 5% DMSO].

In the crystallographic structures for K84L and wild-type dimers, glycerol, which is utilized as cryoprotectant in the crystallization process, is present in the effector-binding site (*22*) with contacts similar to those with IPTG (*23*). Although previous experiments indicate that glycerol is neutral, neither weakening nor enhancing DNA binding (*44*), recent analysis shows that the N-subdomain monomer−monomer interaction network of LacI bound to inducer (IPTG) is similar to that of LacI bound to glycerol (*23*). We have confirmed experimentally that glycerol is a neutral compound and does not

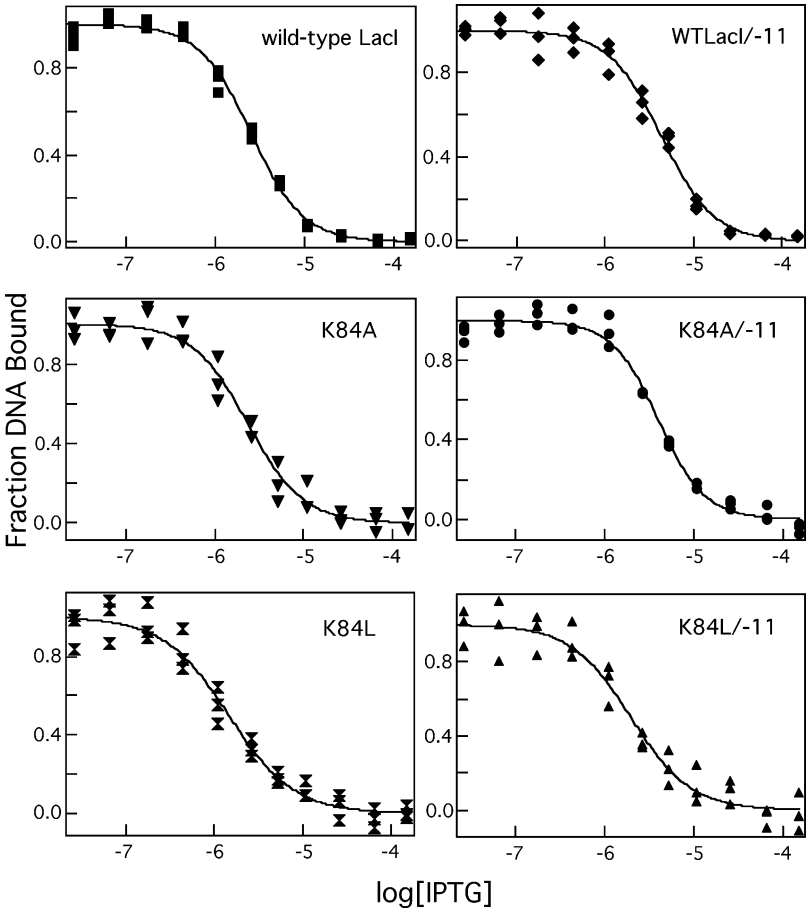

FIGURE 4: Operator release by IPTG of the wild type, K84 variants, and their dimeric versions. These experiments were performed in 0.01 M Tris-HCl (pH 7.4), 0.15 M KCl, 0.3 mM DTT, 0.1 mM EDTA, and 5% DMSO. In the experiments shown, the operator concentration was 1.5×10^{-12}, and protein concentrations were as follows: 2.4×10^{-10} M for the wild type, 7.5×10^{-9} M for WT LacI/−11, 5.2×10^{-10} M for K84A, 3.2×10^{-9} M for K84A/−11, 2.5×10^{-9} M for K84L, and 2.4×10^{-9} M for K84L/−11. Data from a single experiment are shown, and the results from multiple measurements are summarized in Table 4. Although the effect of DNA on K84L IPTG binding is small, the difference is repeatable over multiple assays.

affect DNA binding at the extremely high concentration used for crystallization (data not shown).

Allosteric Response of K84 Variants. Thermodynamically, allostery is indicated when affinity for one ligand is altered in the presence of a second ligand. For wild-type and −11 LacI, the level of DNA binding is diminished up to 1000-fold in the presence of a saturating IPTG concentration (depending upon buffer conditions, see below; Table 3) (*12*). Likewise, inducer binding is decreased ∼10-fold in the presence of a saturating operator concentration (Table 4), and inducer binding becomes cooperative (*12*, *35*, *39*). Since the effect of IPTG on operator affinity has not been established for K84L and K84A variants, this experiment was undertaken with an extended incubation time to allow association of the inducer and establishment of equilibrium (Tables 3 and 4 and Figures 2 and 4). The difference between DNA binding in the presence and absence of inducer is significantly smaller for the K84 variants (∼5-fold) than for wild-type LacI or the −11 dimer (>1000-fold). Nonetheless, a clear change in operator affinity is generated by the presence of IPTG, suggesting that an allosteric conformational change occurs.

Inducer binding was also examined for these proteins (Figure 3 and Table 4). Again, the effect of O^1 operator DNA on IPTG binding is diminished for the K84 variants compared to wild-type and −11 proteins, but allosteric

Table 4: Inducer Binding of K84 Variants[a]

	IPTG binding[b]			
	K_d ($\times 10^6$ M)	with O^1 DNA	+DNA/−DNA	operator release[c] $[IPTG]_{mid}$ ($\times 10^6$ M)
WT	1.2 ± 0.1	18 ± 10	15 ± 1.4	2.9 ± 0.6
K84A	1.4 ± 0.2	1.9 ± 0.2	1.4 ± 0.2	2.3 ± 0.6
K84L	1.4 ± 0.2	2.1 ± 0.3	1.5 ± 0.3	1.7 ± 0.2
−11	1.3 ± 0.1	44 ± 0.5	34 ± 2.6	4.4 ± 0.5
K84A/−11	1.5 ± 0.1	3.9 ± 0.1	2.6 ± 0.2	4.7 ± 0.9
K84L/−11	1.4 ± 0.4	2.1 ± 0.2	1.5 ± 0.4	2.6 ± 1.5

[a] Standard deviations shown represent a minimum of three measurements and up to six measurements. [b] Sugar binding was assessed in a buffer containing 0.01 M Tris-HCl (pH 7.4) and 0.15 M KCl by fluorescence spectroscopy as described in Materials and Methods. The protein concentration was below 1.5×10^{-7} M monomer. [c] Operator release was monitored in a buffer containing 0.01 M Tris-HCl (pH 7.4), 0.15 M KCl, 0.3 mM DTT, 0.1 mM EDTA, and 5% DMSO. The operator concentration was 1.5×10^{-12} M, and protein concentrations were as follows: 2.4×10^{-10} M for the wild type, 5.2×10^{-10} M for K84A, 2.5×10^{-9} M for K84L, 7.5×10^{-9} M for WT LacI/−11, 3.2×10^{-9} M for K84A/−11, and 2.9×10^{-9} M for K84L/−11,. Alternatively, the operator concentration was 4.8×10^{-11} M for K84A, 4.8×10^{-10} M for K84L, 1×10^{-9} M for K84A/−11, and 3×10^{-9} M for K84L/−11; the protein concentration was 0.6×10^{-11} M for K84A, 1.6×10^{-10} M for K84L, 3.3×10^{-10} M for K84A/−11, and 1×10^{-9} M for K84L/−11. Both experimental designs yielded similar values and are included in the averages that are presented (see Materials and Methods). For K84 variants, the incubation time was varied from 1.5 to 27 h and had no effect on the value that was determined.

communication does occur. In contrast to the decreased effects of IPTG on DNA binding, the effects of an anti-inducer on K84 variants were found to be similar to those of wild-type LacI: ONPF increases the operator binding affinity of K84 variants (tetramer and dimer) by ~2-fold (Table 3). Thus, both neutral (glycerol) and anti-inducing (ONPF) small molecule ligands have the same effect on wild-type and K84L/A DNA binding affinity.

Given that the allosteric response is diminished, we turned to other experiments to differentiate between whether the substitutions mute the wild-type response or if they generate a novel allosteric mechanism. Operator release experiments directly detect inducer impact on DNA binding and are affected by all processes (including conformational alterations) that occur between the events of inducer binding and operator release. If the allosteric mechanism changes in the K84 variants, one could expect results from these experiments to differ from wild type. The absolute value of the signal change is smaller for the variants, consistent with equilibrium binding studies. However, the value for $[IPTG]_{mid}$ is very similar to that of the wild type (Table 4 and Figure 4), suggesting that intermediate processes affecting this value are the same. These results are consistent with idea that allostery is damped in the variants rather than different in character.

UV Difference Spectra of K84 Variants. If the binding and allosteric mechanisms are similar in the wild type and K84 variants, the changes in response to inducer binding detected by UV difference spectroscopy should be similar. Inducer binding affects the environment of multiple LacI aromatic residues (mainly tryptophan and tyrosine). Effects on a subset of specific, dominant tryptophan features reflect direct contact, whereas other spectral characteristics derive from environmental changes consequent to the conformational shift (*26*, *28*−*30*, *37*, *45*). For IPTG, wild-type LacI difference spectra have unique minima at 280, 288, and 308 nm (Figure 5). The UV difference spectra of K84L/−11 and K84A/−11 have similar, but not identical, features. To ensure the absence of kinetic effects, the spectral data were found to be unaltered after incubation times of up to 24 h. The minima at 280 and 288 nm are deeper than those of wild-type LacI, with consistently different features between 290 and 300 nm. However, these characteristics are not novel; they are also observed in difference spectra for other LacI variants (S77L and S151P) with altered allosteric properties (*26*, *46*). Thus, these signals, while dominated by inducer contacts, may report on different regions of the structure that can be mechanistically separated during allostery.

Kinetic Measurements of K84 Variants. Given that the K84 variants respond to inducer in a manner that is largely similar to that of wild-type LacI, albeit reduced in magnitude, these mutant proteins provide a unique opportunity to test the hypothesis that a LacI dimer must bind two inducer molecules to release the operator. Inducer binding kinetics for these mutants are extremely slow compared to those of wild-type LacI and are biphasic, with the second phase an order of magnitude slower than the first (*20*). Thus, our strategy was to compare the rate constants of inducer binding in the presence of operator DNA with the rate constant for operator release. We expected the kinetics of operator release would match the kinetics of the inducer binding event (first or second) required to effect the allosteric change.

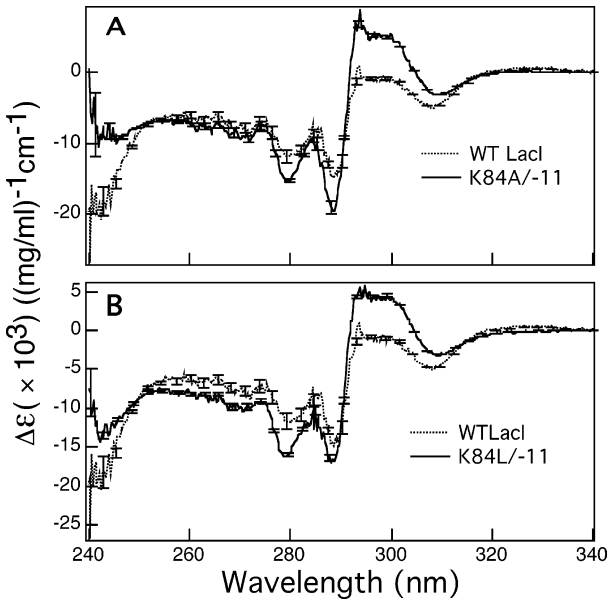

FIGURE 5: UV difference spectra in response to IPTG binding. Difference spectra were measured at room temperature in a buffer containing 0.01 M Tris-HCl (pH 7.4) and 0.15 M KCl. Protein was placed in one chamber of a split quartz cuvette, and a precisely equal volume of 1.0 mM IPTG was added to the other chamber. After the volumes were mixed, the final concentration of IPTG was exactly half the initial concentration, whereas the effective path length for the mixed solution doubled. The spectra are reported as the change in the absorption coefficient. The difference spectra were determined by subtracting the average of three spectra for the unmixed apoprotein from the average of three spectra for the mixed, inducer-bound protein. Panels A and B show the spectra obtained for wild-type LacI, K84A/−11, and K84L/−11 as indicated.

Operator release is a complicated process involving inducer binding, allosteric transition, and vacation of operator. To avoid further complication from possible dissociation of dimeric LacI variants, tetrameric versions of K84A and K84L were utilized. Since previous experiments determined inducer binding kinetics only in the absence of operator, we first measured IPTG binding kinetics in the presence of DNA via the fluorescence signal change that occurs upon addition of IPTG (Figure 6A,E). Data were fit using a double-exponential transition (eq 5) to yield two observed association rates. To determine the microscopic association rate constants (Table 5), the rates at multiple concentrations of IPTG were measured and analyzed (eq 4) (Figure 6B,C,F,G). As a control, the rate constants for inducer binding in the absence of operator DNA were measured and are in reasonable agreement with data reported previously for K84 variants (*20*) (Table 5).

For inducer binding to the wild-type LacI−operator complex, k_{on} was diminished ~5-fold compared to that of the unliganded repressor (*47*). (Note that this event is described by a single exponential.) However, for K84A or K84L bound to operator DNA, the faster association rate constants are increased, whereas the slower ones are comparable to those in the absence of operator DNA (Table 5). These changes separate further the two binding events in time. Dissociation rate constants were also measured for the complex of IPTG with K84A and K84L in the absence and presence of operator DNA (Figure 6D,H). The dissociation kinetics are also biphasic and slow compared to those for wild-type LacI (Table 5), as required for the generation of

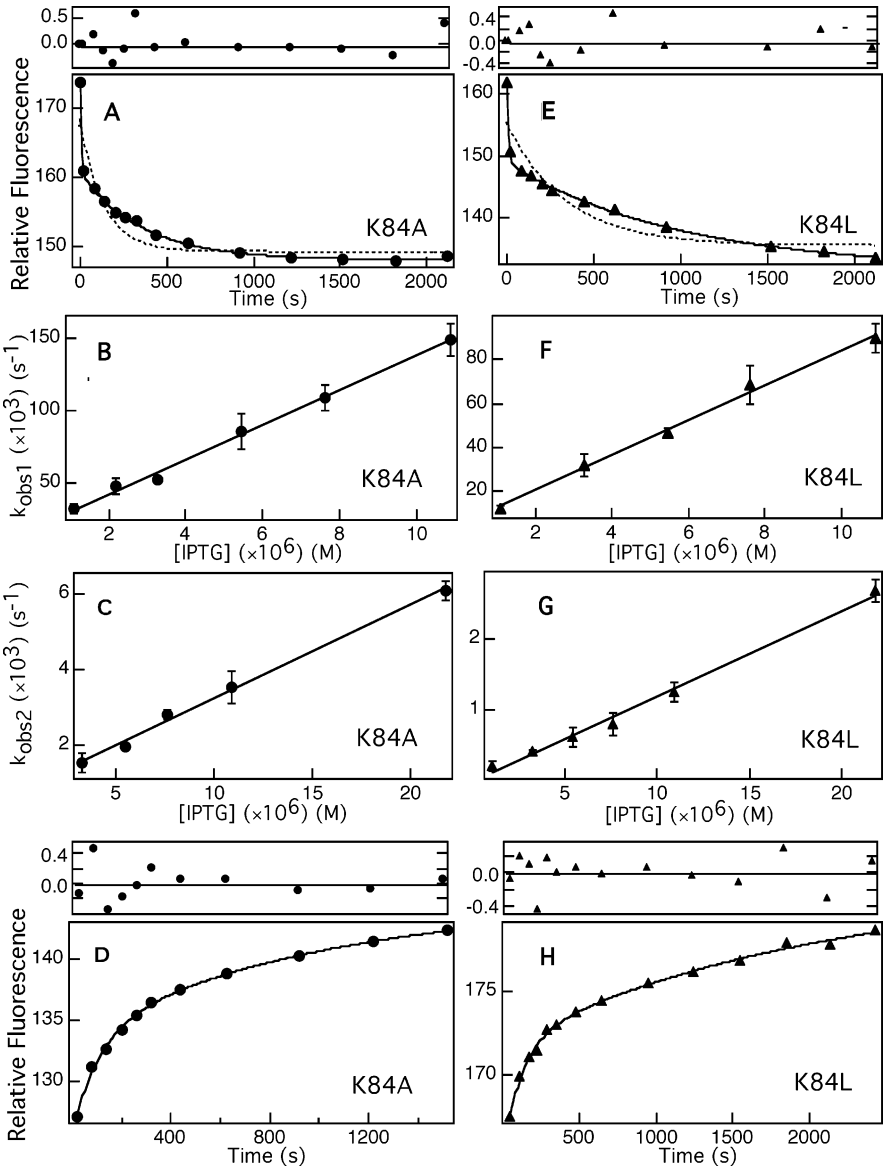

FIGURE 6: Inducer binding kinetics of K84A and K84L in the presence of operator. Panels A and E show the fluorescence signal intensities recorded at different times after mixing protein and IPTG. The protein concentration was 5×10^{-7} M in monomer. The operator O^1 concentration was 1×10^{-6} M. Panel A shows the binding kinetics of K84A upon addition of 7.6×10^{-6} M IPTG, and panel E is for the binding of K84L upon addition of 1.1×10^{-5} M IPTG. The curves were fit to a double-exponential transition (eq 5). In panels B, C, F, and G, the two sets of observed association rates are plotted vs IPTG concentration and fit with a linear model to calculate the two association rate constants (eq 4). Data are shown for one set of IPTG concentrations, and the results from multiple sets are summarized in Table 5. The dashed lines in panels A and E show that a single-exponential model does not fit the curves as well as the double-exponential model. Residuals for double-exponential fits are provided at the top of the figure. Panels D and H show the biphasic IPTG dissociation rate measurements for K84A and K84L determined by fluorescence spectroscopy as described in Materials and Methods. The protein·PTG complex was formed by incubating 2.5×10^{-6} M (monomer) proteins and 8×10^{-6} M IPTG for ~35 min, followed by dilution to assess dissociation.

equilibrium binding constants for IPTG similar to those of wild-type LacI.

For wild-type LacI, operator release kinetics are too fast to measure (data not shown). However, the slowed kinetics of IPTG binding for the K84 variants resulted in slowed operator release. Release data for K84L and K84A were fit readily by a single-exponential transition (Figure 7A,C). The observed transitions were also fit using double-exponential models (data not shown); these fits yielded similar observed rates with a second value for the double exponential similar to the first. The release rates at varying concentrations of IPTG were utilized to determine an intrinsic "releasing" rate constant (Figure 7B,D). These data indicate that release of operator DNA occurs in response to a single process, presumably the binding of a specific IPTG molecule. Importantly, the releasing rate constant matches most closely the slower association rate constant for inducer binding to K84A and K84L (Table 5). Thus, binding two IPTG molecules per dimer appears to be required to elicit the conformational change that releases operator for these mutants.

DISCUSSION

Although allosteric protein behavior is required for many biological processes, the detailed atomic-level mechanism is not well understood for most proteins. Crystallographic structures of LacI facilitate our understanding of the allosteric mechanism in this protein, but provide information only

Table 5: Kinetic Rate Constants for K84A and K84L[a]

	IPTG binding (M^{-1} s^{-1})[b]	IPTG binding with O^1 DNA (M^{-1} s^{-1})[c]	operator release (M^{-1} s^{-1})[d]	IPTG dissociation ($\times 10^3$ s^{-1})	IPTG dissociation with O^1 DNA ($\times 10^3$ s^{-1})
K84A	6600 ± 430	11000 ± 530		4.5 ± 0.3	11 ± 1.5
	260 ± 28	**260 ± 54**	**240 ± 31**	0.54 ± 0.09	1.2 ± 0.2
K84L	2200 ± 140	8100 ± 670		3.8 ± 1.3	8.0 ± 0.2
	76 ± 13	**120 ± 17**	**200 ± 22**	0.47 ± 0.09	0.4 ± 0.1

[a] Standard deviations shown represent a minimum of three measurements and up to four measurements. [b] IPTG binding kinetics were monitored in a buffer containing 0.01 M Tris-HCl (pH 7.4) and 0.15 M KCl. [c] For IPTG binding kinetics in the presence of DNA, the O^1 concentration was 1×10^{-6} M. [d] Operator release kinetics were monitored in a buffer including 0.01 M Tris-HCl (pH 7.4), 0.15 M KCl, 0.3 mM DTT, 0.1 mM EDTA, 5% DMSO, and 0.2 mg/mL BSA. The protein concentration was 2.7×10^{-11} M for K84A and 1.6×10^{-10} M for K84L. The operator O^1 concentration was 8.1×10^{-11} M for K84A and 4.8×10^{-10} M for K84L.

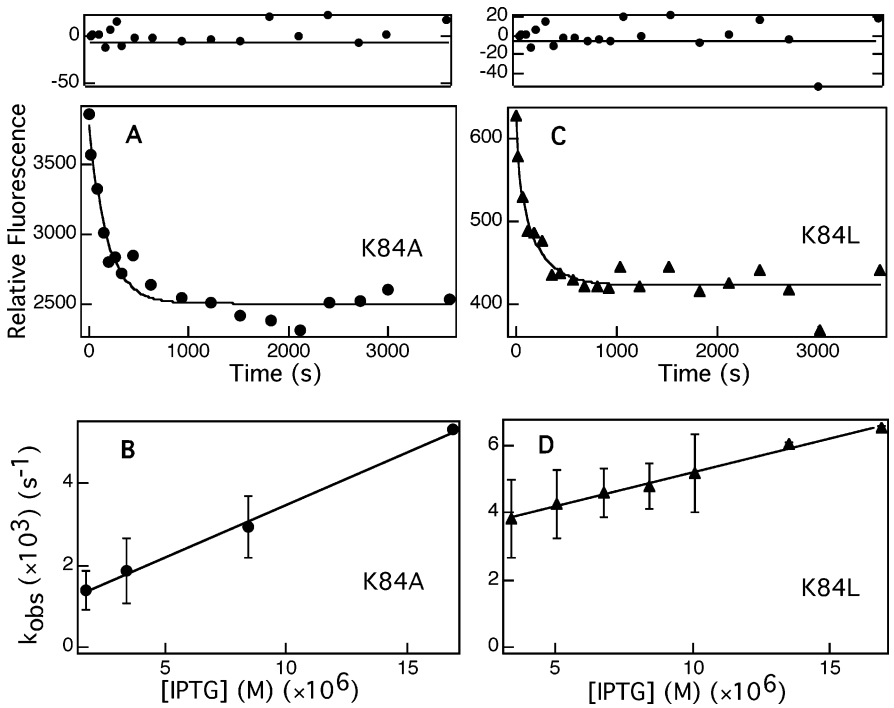

FIGURE 7: Operator release kinetics for K84A and K84L. Panels A and C show the retained radioactivity at different times after mixing the protein−operator complex and IPTG. Before being mixed with IPTG, protein was incubated with operator DNA for ~50 min. Panel A shows the operator release for K84A by 1.1×10^{-5} M IPTG, whereas panel C is for the release of K84L by 1.1×10^{-5} M IPTG. The protein concentration was 2.7×10^{-11} M for K84A and 1.6×10^{-10} M for K84L. The operator O^1 concentration was 8.1×10^{-11} M for K84A and 4.8×10^{-10} M for K84L. The curves were fit by a single-exponential transition (eq 3). In panels B and D, the observed rates were plotted vs IPTG concentration and fit with a linear model to calculate a rate constant (eq 4). Data are shown for one set of IPTG concentrations, and the results from multiple ($n \geq 3$) sets are summarized in Table 5. As indicated in the text, a double-exponential transition yielded values for both phases similar to the single-exponential transition. Residuals for single-exponential fits are provided at the top of the figure.

about three end states (repressed, apo, and induced) (*2*−*4*, *19*, *48*), with minimal insight into the detailed transition between them. Thus, identification and characterization of intermediates along the LacI allosteric pathway have emerged as a key priority.

Two approaches may be taken to achieve this aim: (a) trapping intermediates via mutation or (b) using recently developed computational methods [e.g., TMD (*1*, *5*)] to simulate the allosteric transition. The problem associated with the first method is assessing whether the identified intermediate is pertinent to the wild-type protein. Likewise, the second approach has the challenge of agreement between the simulation and experimental data. However, concordance between the two techniques can strongly suggest that the mutationally generated intermediate is relevant to the wild-type mechanism. In the recent TMD study of the LacI allosteric transition, three atomic-level pathways were documented. Importantly, the identities of residues involved in the simulated transition are in good agreement with decades of biochemical and genetic study (*3*, *5*, *13*, *14*, *20*, *21*, *49*, *50*). Simulations predicted that the transition of this homodimer is asymmetric, an arrangement that is difficult to verify experimentally. However, review of the LacI literature identified at least two experimental occurrences of biphasic function: K84 hydrophobic variants and S77L (Table 1) (*20*, *46*).

Of the two positions, K84 has been most extensively studied. Early sequence comparisons along with genetic analyses led to the proposal that K84 directly binds inducer (*50*, *51*). In vitro mutational analysis to generate K84A, K84D, K84L, and K84R eventually disproved this hypothesis and suggested that K84 was at a subunit interface (*20*), an arrangement verified by subsequent X-ray crystallographic structures (*2*−*4*). In the operator-bound state, K84 is buried inside the N-subdomain monomer−monomer interface, whereas the side chain reorients and is solvent-exposed in

the inducer-bound state (Figure 1). Mutating this polar residue to a hydrophobic side chain (K84L and K84A) enhances the stability of this interface and can even rescue the assembly defect of Y282D, a monomeric mutation (*11*, *20*, *21*). A distinct property of K84L and K84A variants is slow and biphasic inducer binding (*20*). Thus, these mutations might slow the conformational change so that the asymmetry predicted by TMD can be experimentally observed.

However, allosteric communication of K84A and K84L had not been examined directly. Indeed, in the context of phenotypic results (*49*, *50*), an equally probable hypothesis is that allostery is abolished in these constructs. Results presented herein (Tables 3 and 4) demonstrate that the allosteric response does occur in K84 variants, but is diminished. In addition, ultraviolet difference spectra elicited by IPTG binding are largely similar for wild-type LacI and K84 variants, indicating that binding contacts and the structural change in response to inducer binding remain similar. Contributing further to the view that significant structural changes accompany inducer binding even in the hydrophobic mutants at position 84, recent crystallization trials with the K84L/-11•operator complex in our laboratory have yielded small crystals. These structures cracked and disintegrated in the presence of IPTG, consistent with a significant structural alteration associated with IPTG binding for this LacI variant. Interestingly, the anti-inducer ONPF, which is bound in the same effector site as IPTG, has comparable effects on both wild-type and K84 mutant LacI−operator binding, ~2-fold increase, suggesting the possibility that these ligand effects are distributed via distinct through-protein mechanisms, as recently hypothesized (*23*).

Confirmation that the K84A and K84L conformation changes are relevant to wild-type LacI must await structures of the apo-, DNA-, and inducer-bound states of these variants. At this time, only one structure is available for K84L, that for the dimeric version bound to glycerol, which was confirmed in our studies to be a neutral ligand. Interestingly, the K84L dimer structure incorporates features that occur separately in the wild-type conformations (Table 2). When this information is reconciled with biochemical data, the leucine side chains appear to have a dual affect: (a) sterically blocking the wild-type conformational change of the N-subdomains so that the allosteric response is diminished and (b) removing the energetic impetus (via increasing the hydrophobicity in all conformations; see below) to adopt the inducer-bound state so that the full allosteric response is impeded. The nature of the N-subdomain interface and orientations of the K84 side chain in the inducer-bound complex will be a most interesting addition to this story.

Since current evidence is consistent with a muted but wild-type allosteric response, we used the K84 variants to explore how many inducer molecules must bind a LacI dimer to release DNA. Operator release experiments contain the thermodynamic contribution of IPTG binding to the LacI•O complex as well as the intervening conformational change, but historically, these data have been very difficult to interpret because the dimer-bound operator could be vacated by binding either the first inducer molecule, the second, or both. We noticed that for many LacI variants (*26*, *34*), the midpoint of operator release ($[IPTG]_{mid}$) is consistently only ~2-fold higher than the K_d value for inducer binding in the absence of DNA ($\sim 10^{-6}$ M; Table 6). However, if the first inducer molecule is able to release DNA, one would expect $[IPTG]_{mid}$ to mirror the weaker K_d measured in the presence of DNA ($\sim 10^{-5}$ M). Thus, the midpoint of operator release is too small to represent the first IPTG binding event and suggests an alternate scenario: IPTG binding in the presence of DNA diminishes affinity 10-fold, but the Hill coefficient (*n*) for binding also increases (see Figure 3). Positive cooperativity means that the second IPTG molecule binds the LacI dimer tighter than the first. Thus, the lower value for operator release may actually reflect binding of the second, tighter molecule. The unique kinetic properties of K84A and K84L provide the opportunity to test this idea, linking a specific inducer binding event and operator release. Because their inducer binding is sufficiently slow and biphasic, operator release kinetics can be compared directly to those of the two inducer binding events. Indeed, the measured rate of operator DNA release correlates directly with the slower kinetic constant for inducer binding. Thus, the hypothesis that both IPTG binding sites of a dimer must be occupied to release DNA is supported.

Table 6: Inducibility of LacI Variants

protein	IPTG binding K_d ($\times 10^6$ M)[c]	operator release $[IPTG]_{mid}$ ($\times 10^6$ M)[d]	$[IPTG]_{mid}/K_d$
WT	1.2 ± 0.1	2.9 ± 0.6	2.4 ± 0.3
K84L	1.4 ± 0.2	1.7 ± 0.2	1.2 ± 0.2
K84A	1.4 ± 0.2	2.3 ± 0.6	1.6 ± 0.3
L148F[a]	0.4 ± 0.1	0.7 ± 0.1	1.8 ± 0.5
S151P[a]	4.5 ± 0.8	6.9 ± 1.3	1.5 ± 0.3
P320A[a]	1.0 ± 0.2	3.1 ± 1.8	3 ± 0.9
Q60G/L148F[a]	0.4 ± 0.1	0.8 ± 0.2	2 ± 0.6
Q60G[a,e]	1.5 ± 0.3	2.9 ± 1.1	1.9 ± 0.5
R197G[b]	1200 ± 500[b]	2100	1.8 ± 0.7

[a] From ref *26*. [b] From ref *34*; the operator release value was estimated. [c] IPTG binding affinity was measured in a buffer containing 0.01 M Tris-HCl (pH 7.4) and 0.15 M KCl, which is not the same as that in operator release experiments (see below). Preliminary experiments show that IPTG binding and the midpoint of operator release converge to the same value when determined in the same buffer (*53*). [d] Operator release experiments were performed in a buffer containing 0.01 M Tris-HCl (pH 7.4), 0.15 M KCl, 0.3 mM DTT, 0.1 mM EDTA, and 5% DMSO. [e] From ref *36*.

At least two other LacI variants that have been characterized biochemically increase hydrophobicity at the N-subdomain interface. Asymmetric biochemical function was also observed for the hydrophobic variant S77L as two separate phases for equilibrium inducer binding (*46*). This variant exhibits greatly weakened DNA binding affinity under all circumstances (*46*). Position 77 undergoes important changes in the allosteric pathway identified by TMD and is closely linked to changes at position 84. S77L may actually stabilize an intermediate in the allosteric transition where only one subunit has changed its conformation. A third instance of a hydrophobic mutation having a profound effect on allostery is A81V (Figure 1) (*52*). A81 makes extensive contacts in the N-subdomain interface, and A81V greatly diminishes DNA binding and appears to lock the core domain in an induced conformation (*52*). Thus, the enhanced hydrophobic character of the K84A, K84L, S77L, and A81V interfaces may impede the dynamic behavior required for normal LacI function, either slowing the allowed conformational change or blocking it entirely.

From these collective observations, a fully functional N-subdomain interface appears to require a delicate balance of charged and hydrophobic residues. The charged side chain (K84) may act as a toggle, inserting into the otherwise hydrophobic interface in the DNA-bound state and moving out to solvent in the inducer-bound interface. For the wild-type repressor, increased hydrophobicity in this interface appears to be a driving force in induction. Enhanced hydrophobicity (such as the A81V and S77L substitutions) may prevent insertion of the lysine toggle so that the protein remains in an induced state. With apolar side chains at K84, the protein both loses the toggle and appears to be fixed in a conformation that inhibits the full transition to the inducer-bound form. Nonetheless, significant structural changes in the K84 variants occur in response to inducer that allow correlation of DNA release with the binding of the second IPTG to the dimeric DNA binding unit.

ACKNOWLEDGMENT

We thank Dr. Sarah Bondos for reading the manuscript and the Matthews laboratory for helpful discussion.

REFERENCES

1. Schlitter, J., Engels, M., Kruger, P., Jacoby, E., and Wollmer, A. (1993) Targeted molecular dynamics simulation of conformational change: Application to the T−R transition in insulin, *Mol. Simul. 10*, 291−308.
2. Friedman, A. M., Fischmann, T. O., and Steitz, T. A. (1995) Crystal structure of *lac* repressor core tetramer and its implications for DNA looping, *Science 268*, 1721−1727.
3. Lewis, M., Chang, G., Horton, N. C., Kercher, M. A., Pace, H. C., Schumacher, M. A., Brennan, R. G., and Lu, P. (1996) Crystal structure of the lactose operon repressor and its complexes with DNA and inducer, *Science 271*, 1247−1254.
4. Bell, C. E., and Lewis, M. (2000) A closer view of the conformation of the Lac repressor bound to operator, *Nat. Struct. Biol. 7*, 209−214.
5. Flynn, T. C., Swint-Kruse, L., Kong, Y., Booth, C., Matthews, K. S., and Ma, J. (2003) Allosteric transition pathways in the lactose repressor protein core domain: Asymmetric motions in homodimer, *Protein Sci. 12*, 2523−2541.
6. Matthews, K. S., and Nichols, J. C. (1998) Lactose repressor protein: Functional properties and structure, *Prog. Nucleic Acid Res. Mol. Biol. 58*, 127−164.
7. Jobe, A., and Bourgeois, S. (1972) *lac* Repressor Operator Interaction. VI. The natural inducer of the *lac* operon, *J. Mol. Biol. 69*, 397−408.
8. O'Gorman, R. B., Dunaway, M., and Matthews, K. S. (1980) DNA binding characteristics of lactose repressor and the trypsin-resistant core repressor, *J. Biol. Chem. 255*, 10100−10106.
9. Laiken, S. L., Gross, C. A., and von Hippel, P. H. (1972) Equilibrium and kinetic studies of *Escherichia coli lac* repressor-inducer interactions, *J. Mol. Biol. 66*, 143−155.
10. Chen, J., and Matthews, K. S. (1994) Subunit dissociation affects DNA binding in a dimeric *lac* repressor produced by C-terminal deletion, *Biochemistry 33*, 8728−8735.
11. Barry, J. K., and Matthews, K. S. (1999) Thermodynamic analysis of unfolding and dissociation in lactose repressor protein, *Biochemistry 38*, 6520−6528.
12. Daly, T. J., and Matthews, K. S. (1986) Allosteric regulation of inducer and operator binding to the lactose repressor, *Biochemistry 25*, 5479−5484.
13. Barry, J. K., and Matthews, K. S. (1999) Substitutions at histidine 74 and aspartate 278 alter ligand binding and allostery in lactose repressor protein, *Biochemistry 38*, 3579−3590.
14. Bell, C. E., and Lewis, M. (2001) Crystallographic analysis of Lac repressor bound to natural operator O^1, *J. Mol. Biol. 312*, 921−926.
15. Spronk, C., Bonvin, A., Radha, P. K., Melacini, G., Boelens, R., and Kaptein, R. (1999) The solution structure of Lac repressor headpiece 62 complexed to a symmetrical *lac* operator, *Structure 7*, 1483−1492.
16. Spronk, C. A., Slijper, M., van Boom, J. H., Kaptein, R., and Boelens, R. (1996) Formation of the hinge helix in the *lac* repressor is induced upon binding to the *lac* operator, *Nat. Struct. Biol. 3*, 916−919.
17. Kalodimos, C. G., Biris, N., Bonvin, A. M., Levandoski, M. M., Guennuegues, M., Boelens, R., and Kaptein, R. (2004) Structure and flexibility adaptation in nonspecific and specific protein-DNA complexes, *Science 305*, 386−389.
18. Kalodimos, C. G., Bonvin, A. M., Salinas, R. K., Wechselberger, R., Boelens, R., and Kaptein, R. (2002) Plasticity in protein-DNA recognition: *lac* repressor interacts with its natural operator O1 through alternative conformations of its DNA-binding domain, *EMBO J. 21*, 2866−2876.
19. Bell, C. E., and Lewis, M. (2001) The Lac repressor: A second generation of structural and functional studies, *Curr. Opin. Struct. Biol. 11*, 19−25.
20. Chang, W.-I., Olson, J. S., and Matthews, K. S. (1993) Lysine 84 is at the subunit interface of *lac* repressor protein, *J. Biol. Chem. 268*, 17613−17622.
21. Nichols, J. C., and Matthews, K. S. (1997) Combinatorial mutations of *lac* repressor. Stability of monomer-monomer interface is increased by apolar substitution at position 84, *J. Biol. Chem. 272*, 18550−18557.
22. Bell, C. E., Barry, J., Matthews, K. S., and Lewis, M. (2001) Structure of a variant of *lac* repressor with increased thermostability and decreased affinity for operator, *J. Mol. Biol. 313*, 99−109.
23. Swint-Kruse, L. (2004) Using networks to identify fine structural differences between functionally distinct protein states, *Biochemistry 43*, 10886−10895.
24. Chen, J., and Matthews, K. S. (1992) Deletion of lactose repressor carboxyl-terminal domain affects tetramer formation, *J. Biol. Chem. 267*, 13843−13850.
25. Wycuff, D. R., and Matthews K. S. (2000) Generation of an AraC-*araBAD* Promoter-Regulated T7 Expression System, *Anal. Biochem. 277*, 67−73.
26. Swint-Kruse, L., Zhan, H., Fairbanks, B. M., Maheshwari, A., and Matthews, K. S. (2003) Perturbation from a distance: Mutations that alter LacI function through long-range effects, *Biochemistry 42*, 14004−14016.
27. Falcon, C. M., Swint-Kruse, L., and Matthews, K. S. (1997) Designed disulfide between N-terminal domains of lactose repressor disrupts allosteric linkage, *J. Biol. Chem. 272*, 26818−26821.
28. Matthews, K. S., Matthews, H. R., Theilmann, H. W., and Jardetzky, O. (1973) Ultraviolet difference spectra of the lactose repressor protein, *Biochim. Biophys. Acta 295*, 159−165.
29. Matthews, K. S. (1974) Ultraviolet difference spectra of the lactose repressor protein II. trypsin core protein, *Biochim. Biophys. Acta 359*, 334−340.
30. Gardner, J. A., and Matthews, K. S. (1990) Characterization of two mutant lactose repressor proteins containing single tryptophans, *J. Biol. Chem. 265*, 21061−21067.
31. Riggs, A. D., Bourgeois, S., Newby, R. F., and Cohn, M. (1968) DNA binding of the *lac* repressor, *J. Mol. Biol. 34*, 365−368.
32. Wong, I., and Lohman, T. M. (1993) A double-filter method for nitrocellulose-filter binding: Application to protein-nucleic acid interactions, *Proc. Natl. Acad. Sci. U.S.A. 90*, 5428−5432.
33. Gilbert, W., and Maxam, A. (1973) The nucleotide sequence of the *lac* operator, *Proc. Natl. Acad. Sci. U.S.A. 70*, 3581−3584.
34. Spotts, R. O., Chakerian, A. E., and Matthews, K. S. (1991) Arginine 197 of *lac* repressor contributes significant energy to inducer binding, *J. Biol. Chem. 266*, 22998−23002.
35. Swint-Kruse, L., and Matthews, K. S. (2004) Thermodynamics, protein modification, and molecular dynamics in characterizating lactose repressor protein: Strategies for complex analyses of protein structure−function, *Methods Enzymol. 379*, 188−209.
36. Falcon, C. M., and Matthews, K. S. (1999) Glycine insertion in the hinge region of lactose repressor protein alters DNA binding, *J. Biol. Chem. 274*, 30849−30857.
37. Chang, W.-I., and Matthews, K. S. (1995) Role of Asp^{274} in *lac* Represssor: Diminished sugar binding and altered conformational effects in mutants, *Biochemistry 34*, 9227−9234.
38. Carey, J. (1991) Gel retardation, *Methods Enzymol. 208*, 103−118.
39. O'Gorman, R. B., Rosenberg, J. M., Kallai, O. B., Dickerson, R. E., Itakura, K., Riggs, A. D., and Matthews, K. S. (1980)

Equilibrium binding of inducer to *lac* repressor-operator DNA complex, *J. Biol. Chem. 255*, 10107−10114.
40. Chen, J., Surendran, R., Lee, J. C., and Matthews, K. S. (1994) Construction of a dimeric repressor: Dissection of subunit interfaces in *lac* repressor, *Biochemistry 33*, 1234−1241.
41. Mossing, M. C., and Record, M. T., Jr. (1986) Upstream operators enhance repression of the *lac* promoter, *Science 233*, 889−892.
42. Oehler, S., Eismann, E. R., Krämer, H., and Müller-Hill, B. (1990) The three operators of the *lac* operon cooperate in repression, *EMBO J. 9*, 973−980.
43. Daly, T. J., and Matthews, K. S. (1986) Characterization and modification of a monomeric mutant of the lactose repressor protein, *Biochemistry 25*, 5474−5478.
44. Riggs, A. D., Newby, R. F., and Bourgeois, S. (1970) *lac* repressor-operator interaction II. Effect of galactosides and other ligands, *J. Mol. Biol. 51*, 303−314.
45. O'Gorman, R. B., and Matthews, K. S. (1977) Fluorescence and ultraviolet spectral studies of *lac* repressor modified with N-bromosuccinimide, *J. Biol. Chem. 252*, 3572−3577.
46. Chou, W.-Y., and Matthews, K. S. (1989) Mutation in hinge region of lactose repressor protein alters physical and functional properties, *J. Biol. Chem. 264*, 6171−6176.
47. Dunaway, M., Olson, J. S., Rosenberg, J. M., Kallai, O. B., Dickerson, R. E., and Matthews, K. S. (1980) Kinetic studies of inducer binding to *lac* repressor·operator complex, *J. Biol. Chem. 255*, 10115−10119.
48. Matthews, K. S., Falcon, C. M., and Swint-Kruse, L. (2000) Relieving repression, *Nat. Struct. Biol. 7*, 184−187.
49. Markiewicz, P., Kleina, L. G., Cruz, C., Ehret, S., and Miller, J. H. (1994) Genetic studies of the *lac* repressor. XIV. Analysis of 4000 altered *Escherichia coli lac* repressors reveals essential and non-essential residues, as well as "spacers" which do not require a specific sequence, *J. Mol. Biol. 240*, 421−433.
50. Suckow, J., Markiewicz, P., Kleina, L. G., Miller, J., Kisters-Woike, B., and Müller-Hill, B. (1996) Genetic studies of the Lac repressor. XV: 4000 single amino acid substitutions and analysis of the resulting phenotypes on the basis of the protein structure, *J. Mol. Biol. 261*, 509−623.
51. Sams, C. F., Vyas, N. K., Quiocho, F. A., and Matthews, K. S. (1984) Predicted structure of the sugar-binding site of the *lac* repressor, *Nature 310*, 429−430.
52. Chakerian, A. E., Pfahl, M., Olson, J. S., and Matthews, K. S. (1985) A mutant lactose repressor with altered inducer and operator binding parameters, *J. Mol. Biol. 183*, 43−51.
53. Zhan, H. L. (2005) Biophysical characterization of the allosteric transition in lactose repressor protein (LacI), Ph.D. Thesis, Rice University, Houston.

BI050404+